

Circular Trajectory Approach for Online Sinusoidal Signal Distortion Monitoring and Visualization

Haoyuan Sun¹, Graduate Student Member, IEEE, Fangxing Li², Fellow, IEEE, Christopher Sticht³, Senior Member, IEEE, and Srijib Mukherjee⁴, Senior Member, IEEE

Abstract—The increasing complexity and uncertainties of modern power systems are placing greater demands on signal monitoring techniques. This letter proposes the Circular Trajectory Approach (CTA) for online sinusoidal signal distortion monitoring and visualization. CTA can detect distortions of a sinusoidal signal. Compared with existing waveform anomaly detection techniques, CTA is faster in detection and less computation intensive. It thus supports edge devices and online applications. CTA also offers a new means of sinusoidal signal distortion visualization. It can reveal the distorted sections in a sinusoidal cycle and clearly display the distortions. The proposed approach is tested on real data from an open source EPRI dataset.

Index Terms—Circular trajectory approach (CTA), sinusoidal signal, distortion monitoring, distortion visualization.

I. INTRODUCTION

RECENTLY, with the integration of renewable energy resources, distributed generation, and power electronic device interfaced facilities, modern power systems are becoming larger, more complex and have higher uncertainties. High-resolution point-on-wave (POW) data are recorded for system operation, analysis and planning [1]. However, present monitoring methods are designed based on PMU data, which has a rather low sample rate, typically 60 Hz or one sample per sinusoidal cycle. In addition, PMU data is filtered and processed to yield synchrophasors [1]. This process eliminates some of the valuable information contained in the original waveforms. Limited by the PMU data, it is difficult for present methods to achieve very fine scale monitoring. By contrast, POW data has a much higher sample rate and thus has a much higher resolution. Moreover, POW data is recorded with minimal filtering. Therefore, finer scale monitoring of power system signals is facilitated to cover not only large abnormal conditions like amplitude variations, but also small ones like harmonics or other small fluctuations.

In the present signal monitoring practice, numerous trigger conditions are adopted to detect anomalies and to trigger data recording [2]. For example, pickup value reached, sag or

swell detected, negative or zero sequence component detected, certain frequency component detected, etc. However, power systems are becoming more complex and uncertain. Although more trigger conditions are added, they still cannot cover all potential circumstances, not to mention the large computational burden. As reported in [1], “Some POW devices triggered for related faults but did not specifically trigger for and fully record these PV disconnects.” These anomalies are not detected because there is no specific trigger condition for them. It is beneficial to develop a generic monitoring mechanism that is sensitive to all distortions and use it as a trigger for data recording and a call for further analysis.

Existing waveform anomaly detection techniques are not suitable for online uses. Edge devices only have limited computing power and storage. However, existing techniques like those based on fast Fourier transform (FFT) usually involve complicated computation and require a database of abnormal waveforms, which is mainly because they work on both anomaly detection and classification at the same time. Detection is less complex than classification, and usually more urgent. Thus, it is sensible to separate detection from classification.

Existing techniques usually work on waveform segments, or time windows. This means the detection of any anomaly is delayed by at least the length of these time windows. Further, time windows cause a dilemma between information losses and computational load: small steps and large overlapping captures the most information but greatly increases computation; large steps and no overlapping minimizes computation but lead to significant information losses.

Apart from monitoring, another demand when dealing with signals is visualization. A simple way is to display the signal along the time axis. However, this sinusoidal waveform is hard to follow because it is fluctuating. Distortion of a fluctuating waveform is even harder to catch because there is no reference.

This letter proposes the Circular Trajectory Approach (CTA). It is designed for online sinusoidal signal distortion monitoring and visualization with the following objectives: (1) to achieve finer scale monitoring for sinusoidal signals; (2) to provide a more generic solution and replace the existing numerous trigger conditions; (3) to induce less computation; (4) to focus on anomaly detection; (5) to achieve earlier detection; (6) to avoid using time windows; (7) to offer a new means of sinusoidal signal visualization.

II. THE PROPOSED CIRCULAR TRAJECTORY APPROACH

A. Origin of the Proposed Approach

The idea of this CTA originated from a very simple trigonometric identity.

$$\sin^2(\omega t) + \cos^2(\omega t) = 1. \quad (1)$$

Manuscript received October 7, 2021; revised January 28, 2022; accepted February 12, 2022. Date of publication March 3, 2022; date of current version June 21, 2022. This work was supported by the U.S. Department of Energy, Office of Energy Efficiency and Renewable Energy under Contract DE-AC05-00OR22725. Paper no. PESL-00266-2021. (Corresponding author: Fangxing Li.)

Haoyuan Sun and Fangxing Li are with the Department of Electrical Engineering and Computer Science, The University of Tennessee, Knoxville, TN 37996 USA (e-mail: hsun19@vols.utk.edu; fli6@utk.edu).

Christopher Sticht and Srijib Mukherjee are with the Power Systems Resilience Group, Oak Ridge National Laboratory, Oak Ridge, TN 37830 USA (e-mail: stichtcr@ornl.gov; mukherjeesk@ornl.gov).

Color versions of one or more figures in this article are available at <https://doi.org/10.1109/TSG.2022.3156364>.

Digital Object Identifier 10.1109/TSG.2022.3156364

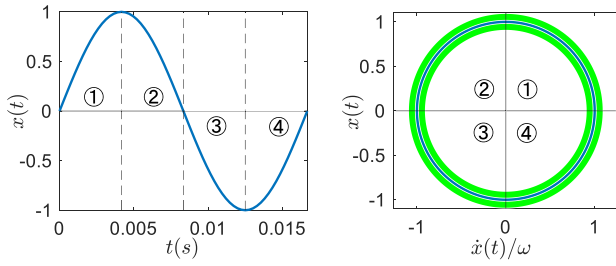


Fig. 1. A perfect sinusoidal signal (left) and its circular trajectory (right).

This identity leads to two thoughts. First, a sinusoidal signal can be transposed to a constant with some simple calculation, which could be useful for monitoring purposes because a constant is obviously much easier to monitor than a sinusoidal signal. Second, the trajectory of two sinusoidal signals, if one leads the other by a quarter cycle, is a circle. This circle could be used for monitoring and visualization purposes.

B. Obtaining Two Sinusoidal Signals

To put the aforementioned two thoughts into practice, two sinusoidal signals are needed. One of these would be, of course, the signal to be monitored. A general sinusoidal signal with amplitude A and initial phase angle φ can be expressed by (2), with frequency fluctuation taken into consideration and denoted as a function of time $\omega(t)$.

$$x(t) = A \sin\left(\int_0^t \omega(\tau) d\tau + \varphi\right) \quad (2)$$

Since the derivative of a sinusoidal signal is still sinusoidal, a simple way to obtain the other sinusoidal signal is to take the derivative of the first one. The derivative of (2) is as follows:

$$\dot{x}(t) = A \cos\left(\int_0^t \omega(\tau) d\tau + \varphi\right) \cdot \omega(t). \quad (3)$$

C. The Proposed Circular Trajectory Approach

By rearranging (2) and (3) into a similar form as (1), the following equation can be obtained.

$$x(t)^2 + (\dot{x}(t)/\omega(t))^2 = A^2 \quad (4)$$

If $x(t)$ is a perfect sine signal, the trajectory of the two sinusoidal terms in Eq. (4), i.e., $x(t)$ and $\dot{x}(t)/\omega(t)$, is a circle in a 2-D plane, as shown in Fig. 1. Therefore, this proposed approach is named the Circular Trajectory Approach. The radius of the circular trajectory is the amplitude of the sine signal.

The circular trajectory of any sinusoidal signal $x(t)$, with or without distortions, can be obtained by plotting $[\dot{x}(t)/\omega(t), x(t)]$ on a 2-D plane. $\dot{x}(t)/\omega(t)$ is deliberately placed along the horizontal axis such that the resulting circular trajectory follows the positive direction of rotation. It can be proven that Eq. (4) should hold if and only if $x(t)$ is a sinusoidal signal. (The proof is in the Appendix.) This means that the circular trajectory of $x(t)$ is a circle if and only if $x(t)$ is a perfect sinusoidal signal.

$$d_{\min} \leq \sqrt{x(t)^2 + (\dot{x}(t)/\omega(t))^2} \leq d_{\max} \quad (5)$$

CTA can be used for sinusoidal signal anomaly detection. Distortions can be detected by comparing the distance from points on the circular trajectory to the origin with a preset normal value. Any deviation from the normal value suggests

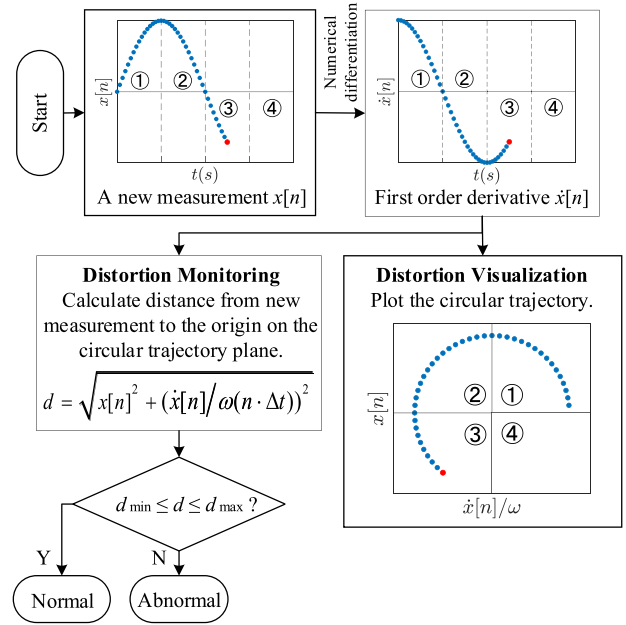


Fig. 2. The workflow of CTA.

distortions in the signal. A threshold range $[d_{\min}, d_{\max}]$, or dead band, can be set around the normal value to accommodate acceptable fluctuations, as shown by inequation (5) and the green circular ring in Fig. 1. Any point falling out of this range is detected as abnormal. The sensitivity can be easily tuned by adjusting the range $[d_{\min}, d_{\max}]$.

CTA can also be used for sinusoidal signal distortion visualization. A fluctuating signal is transposed into a steady circular trajectory, from which a distortion is much easier to catch. A full cycle of a sinusoidal signal can be divided into four sections, which correspond to the four quadrants of the circular trajectory plane, as shown in Fig. 1. The same section of each cycle always corresponds to the same quadrant. This property helps reveal which section of the sinusoidal signal is distorted.

The workflow of CTA is presented in Fig. 2.

For the $\omega(t)$ part in (5), instantaneous frequency measurements could be used. According to [3], frequency measurements with 1440 Hz reporting rate are already available, which is high enough for distortion monitoring purposes.

Using the nominal frequency as an approximation of $\omega(t)$ is also practical. It no longer needs the frequency measurements and thus leads to better simplicity. However, this is at the price of a systematic error. Commonly seen frequency fluctuation is within $\pm 0.5\%$, or ± 0.3 Hz for the nominal frequency of 60 Hz. The largest error for left hand side of Eq. (4) occurs when $\dot{x}(t)$ reaches its maximum $A\omega(t)$ and $\omega(t)$ reaches its minimum $\omega_{\min} = 59.7$ Hz, as given by Eq. (6).

$$\varepsilon_{\max} = \left| (A\omega_{\min}/\omega_{\min})^2 - (A\omega_{\min}/\omega_n)^2 \right| / A^2 = 1\% \quad (6)$$

D. Obtaining the Derivative From Discrete Measurements

In reality, the sinusoidal signal to be monitored is available as a sequence of discrete measurements. A discrete sinusoidal signal and its derivative can be described as follows:

$$x[n] = A \sin\left(\int_0^{n \cdot \Delta t} \omega(\tau) d\tau + \varphi\right), \quad (7)$$

$$\dot{x}[n] = A \cos\left(\int_0^{n \cdot \Delta t} \omega(\tau) d\tau + \varphi\right) \cdot \omega(n \cdot \Delta t). \quad (8)$$

TABLE I
ERROR AND COMPUTING TIME COMPARISON OF
NUMERICAL DIFFERENTIATION FORMULAS

	Max relative err.	Avg. relative err.	Avg. comput. time
2-point formula	4.9%	3.1%	0.87 μ s
3-point formula	0.32%	0.16%	0.88 μ s
5-point formula	0.0006%	0.0003%	1.70 μ s

where Δt is the sampling period, $n \cdot \Delta t$ is the timestamp of the measurement $x[n]$, and $x[0]$ is assumed to be measured at $t = 0$.

Eq. (4) can then be written in discrete form as follows:

$$x[n]^2 + (\dot{x}[n]/\omega(n \cdot \Delta t))^2 = A^2. \quad (9)$$

Numerical differentiation can be used to obtain the derivative of such a sequence of measurements as (7). To determine the numerical differentiation formula to be used, an error and computing time comparison is conducted using a segment of a perfect sine wave. The result is shown in Table I.

High order methods achieve better accuracy but also induce more computation. The 3-point formula, as given by Eq. (10), is adopted here as a trade-off between accuracy and complexity.

$$\dot{x}[n] = (x[n+1] - x[n-1])/2\Delta t \quad (10)$$

According to [5], derivative sensors will be developed and deployed in the future. In that case, the above numerical differentiation process can be saved, and CTA will thus become faster and require even less computation.

E. Dealing With Measurement Noise

Real data inherently contains noise. In this letter, two techniques are designed to deal with it. For detection and monitoring purposes, because noise is always smaller than the distortions of interest, a proper threshold range or dead band $[d_{min}, d_{max}]$ can be set to filter out the noise such that CTA will only react to distortions. For visualization purposes, because noise is random while distortions usually have repeating patterns, it will help to superimpose the circular trajectories of a few consecutive cycles such that the repeating patterns will stand out while random noise becomes much less noticeable. Both techniques will be implemented in Section III.

III. CASE STUDY

In this section, the proposed CTA is tested on real event recordings from an open source EPRI dataset [4]. All experiments are conducted in MATLAB R2019b on a laptop with Intel Core i7-8650U @1.90GHz CPU and 16GB RAM.

A. Revelation of Harmonics

Fig. 3 shows a voltage signal and its circular trajectory. The dead band $[d_{min}, d_{max}]$ is set to $11,180 \text{ V} \pm 5\%$. Any point falling out of this range is detected as abnormal and marked red in Fig. 3. By only looking at the waveform it is very difficult to tell whether this sine wave is distorted and what time the distortion occurs. However, the circular trajectory reveals that the signal is indeed distorted, and the distorted sections are clearly reflected. Results from Fourier analysis as shown in Table II confirms the existence of harmonics. The average runtime of this example is 1.41 μ s.

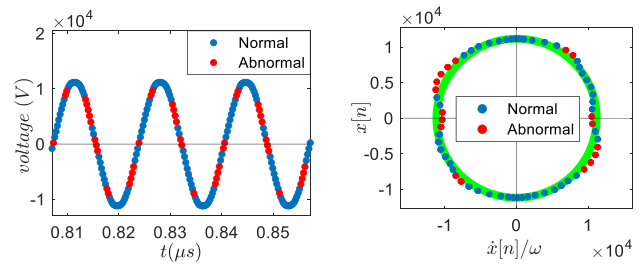


Fig. 3. A voltage signal with harmonics (left) and its circular trajectory (right).

TABLE II
FREQUENCY COMPONENTS OF THE VOLTAGE SIGNAL IN FIG. 3

Frequency Component	Amplitude	Relative Value
60 Hz / 1st order	11,188.42	100%
180 Hz / 3rd order	115.66	1.03%
300 Hz / 5th order	186.71	1.67%
420 Hz / 7th order	37.47	0.33%
540 Hz / 9th order	67.08	0.60%

TABLE III
ERROR COMPARISON OF THE 3-POINT FORMULA
UNDER DIFFERENT SAMPLE RATES

Sample Rate	Max Relative Error	Average Relative Error
6000 Hz	0.13%	0.07%
3840 Hz*	0.32%	0.16%
1920 Hz	1.28%	0.64%
960 Hz	5.04%	2.52%

*The data used in this work has a sample rate of 3840 Hz.

B. Runtime Comparison With FFT

To assess the computational load of CTA, a runtime comparison is conducted. The FFT algorithm is chosen as the benchmark because it is efficient and widely used in signal processing. Theoretically, FFT has a computational complexity of $O(N \log_2 N)$, while CTA has $O(N)$.

The waveform segment presented in Fig. 3 is used for this experiment. The length of the segment is 194. Both algorithms are executed 1 million times to reduce relative error in runtime measurement. FFT took 9.47 s, while CTA took 1.41 s. This verifies that CTA requires much less computation, which makes it more suitable for edge computing than existing techniques.

C. Impact of Sample Rate on CTA

A sufficiently high sample rate is crucial for achieving a satisfying accuracy with numerical differentiation and also for revealing more details of a piece of waveform with CTA. An error comparison of the three-point formula under different sample rates is presented in Table III. The circular trajectories of the same waveform segment in Fig. 3 but with lower sample rates are shown in Fig. 4. With lower sample rates, the trajectories become much less informative. Future grid sensors will have a sample rate of 6000 Hz or higher [5], which is sufficient for satisfactory performance of CTA.

D. Impact of Frequency Variations on CTA

Power systems undergo constant frequency variations. This subsection investigates how this affects CTA. Test signals with frequency variations are generated based on the frequency

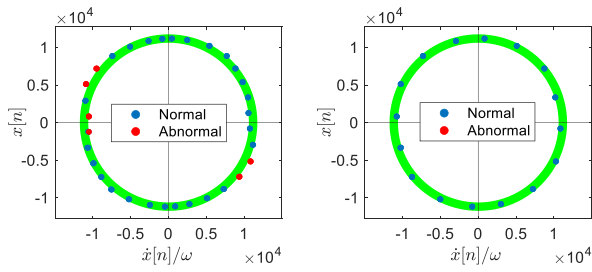


Fig. 4. Circular trajectories of the same waveform segment in Fig. 3 but with lower sample rates, 1920 Hz (left) and 960 Hz (right).

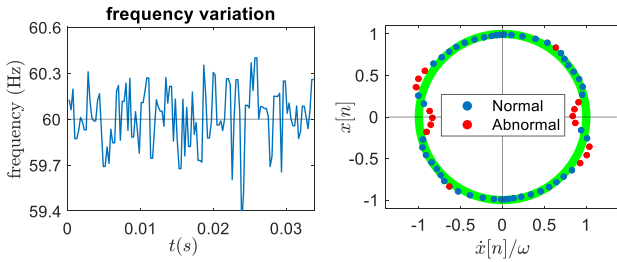


Fig. 5. The circular trajectory of a signal with frequency variations in a commonly seen range, $\pm 0.5\%$ or $60 \pm 0.3\text{Hz}$.

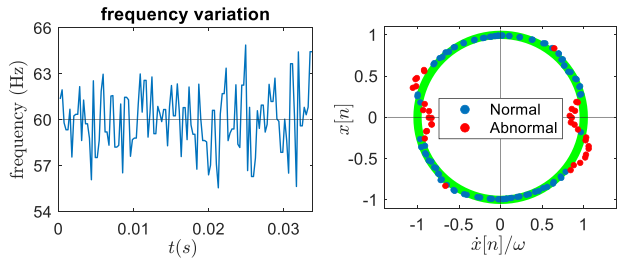


Fig. 6. The circular trajectory of a signal with very large frequency variations, $\pm 5\%$ or $60 \pm 3\text{Hz}$. (Only for test sake. No power system has such large frequency variations.)

components given in Table II to mimic the voltage signal in Fig. 3. By comparing Figs. 4, 5 and 6, it can be concluded that CTA can still detect sinusoidal waveform distortions when the input signal contains frequency variations.

IV. CONCLUSION AND FUTURE WORK

To achieve finer scale and more generic sinusoidal signal monitoring, a Circular Trajectory Approach (CTA) is proposed for sinusoidal signal distortion monitoring and visualization. It can detect distortions of a sinusoidal signal. Furthermore, a dead band can be set to adjust the sensitivity. CTA also offers a new means of sinusoidal signal distortion visualization. It can reveal the distorted

sections in a sinusoidal cycle and clearly display distortions, even small ones. CTA is tested on real data from an open-source EPRI dataset. A runtime comparison study with FFT is conducted. This letter also investigated how sample rate and frequency variation may affect CTA.

Future works include investigation of how the shape of the circular trajectory is related to the order, amplitude and phase angle of the harmonic components, and how CTA may help with anomaly classification.

APPENDIX

Proposition: Eq. (4) holds if and only if $x(t)$ is a sinusoidal signal.

Proof: From equation (4), we can derive:

$$\begin{aligned} dx(t)/dt &= \pm\omega(t)\sqrt{A^2 - x(t)^2} \\ \arcsin(x(t)/A) &= \pm \int \omega(t)dt + C_1 \\ dx(t)/\sqrt{A^2 - x(t)^2} &= \pm\omega(t)dt \\ x(t) &= \pm A \sin(\int \omega(t)dt + C) \end{aligned}$$

Therefore, $x(t)$ is a sinusoidal signal with amplitude A . ■

ACKNOWLEDGMENT

This letter has been authored by UT-Battelle, LLC under Contract No. DE-AC05-00OR22725 with the U.S. Department of Energy. The United States Government retains and the publisher, by accepting this letter for publication, acknowledges that the United States Government retains a nonexclusive, paid-up, irrevocable, world-wide license to publish or reproduce the published form of this letter, or allow others to do so, for United States Government purposes. The Department of Energy will provide public access to these results of federally sponsored research in accordance with the DOE Public Access Plan (<http://energy.gov/downloads/doe-public-access-plan>).

REFERENCES

- [1] A. Silverstein and J. Follum, "High-resolution, time-synchronized grid monitoring devices," North Amer. Synchrophasor Initiative, Washington, DC, USA, Rep. NAPS-2020-TR-004, Mar. 2020. [Online]. Available: <https://www.naspi.org/node/819>
- [2] A. J. Wilson, D. R. Reising, R. W. Hay, R. C. Johnson, A. A. Karrar, and T. D. Loveless, "Automated identification of electrical disturbance waveforms within an operational smart power grid," *IEEE Trans. Smart Grid*, vol. 11, no. 5, pp. 4380–4389, Sep. 2020.
- [3] S. Liu *et al.*, "Model-free data authentication for cyber security in power systems," *IEEE Trans. Smart Grid*, vol. 11, no. 5, pp. 4565–4568, Sep. 2020.
- [4] "DOE/EPRI National Database Repository of Power System Events," EPRI. [Online]. Available: http://pqmon.epri.com/disturbance_library/ (Accessed: Jan. 26, 2022).
- [5] D. T. Rzy, *Sensing and Measurement Technology Roadmap*, U.S. Dept. Energy, Grid Modernization Lab. Consortium, Washington, DC, USA, Feb. 2019.